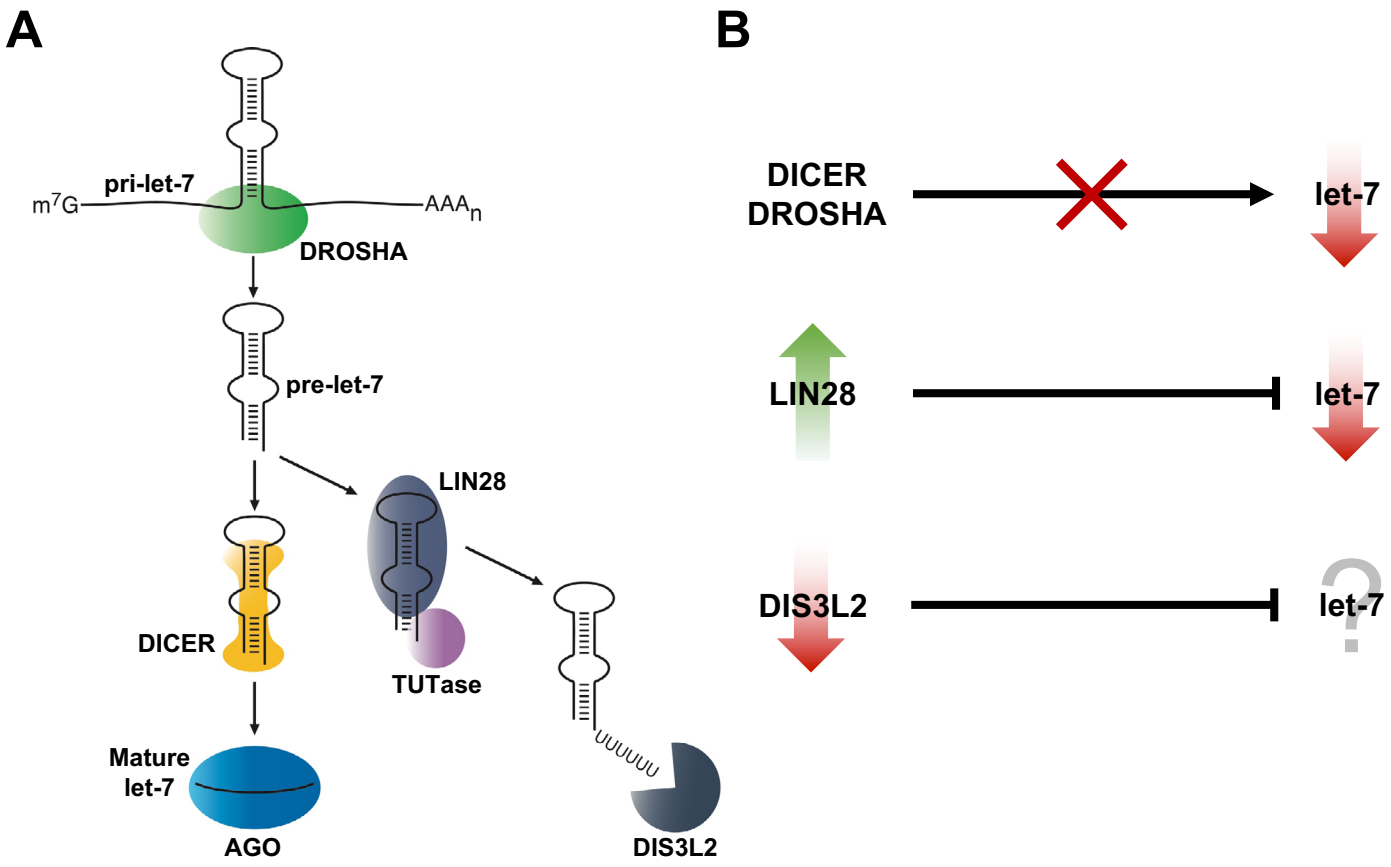

Supplemental Figure S1. The role of DIS3L2 in the LIN28-let-7 pathway. (*A*) Schematic of the LIN28-let-7 pathway, depicting the normal steps in let-7 biogenesis and diversion from this pathway by LIN28, which recruits a terminal uridylyl transferase (TUTase) to pre-let-7, leading to uridylation and subsequent degradation by DIS3L2. (*B*) While mutations in DROSHA or DICER, or overexpression of LIN28, reduce mature let-7 levels, it is unclear how loss of DIS3L2 could influence mature let-7 since uridylated pre-let-7, the relevant DIS3L2 substrate, cannot be further processed into the mature miRNA by DICER.

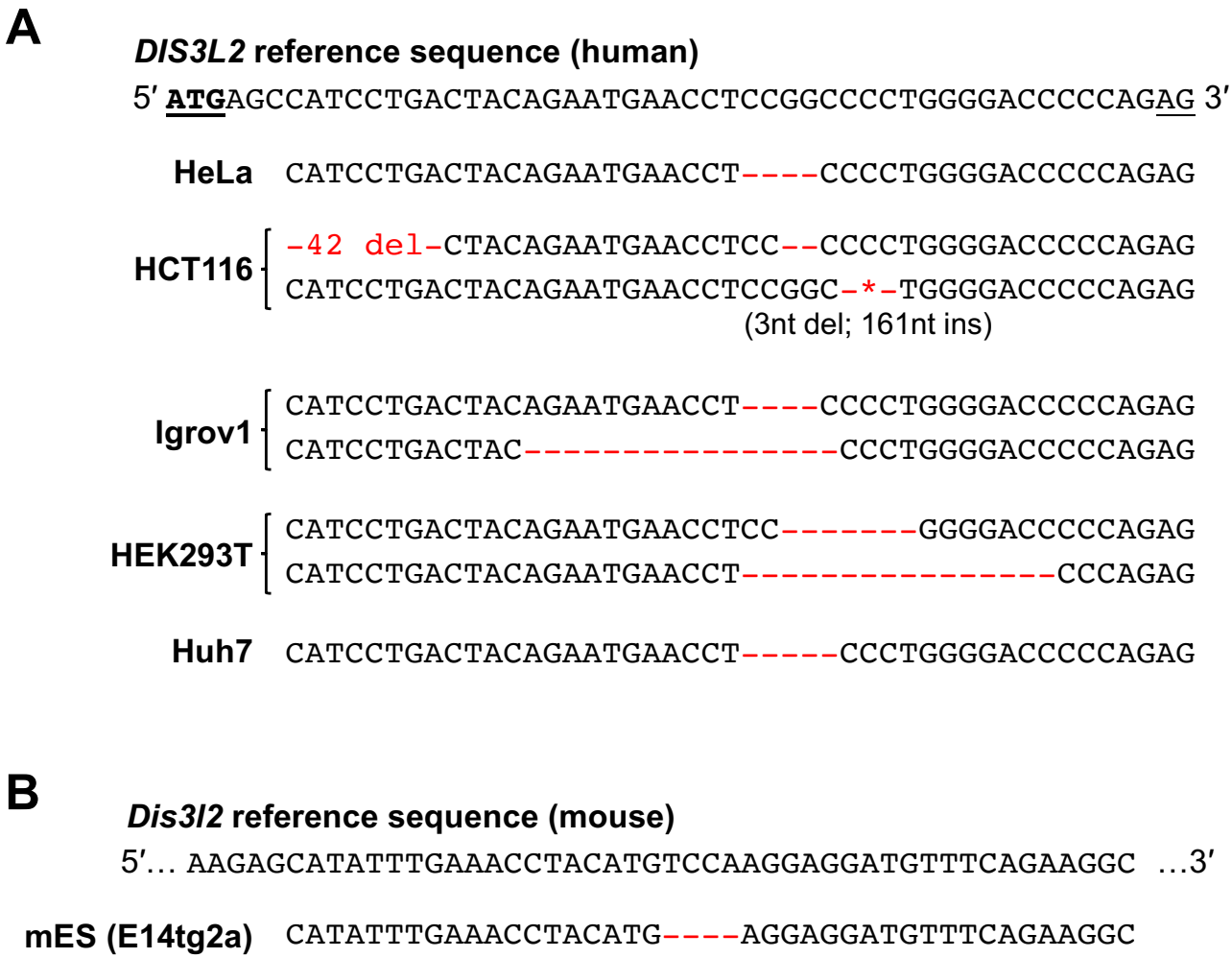

Supplemental Figure S2. Sequence of gene-edited alleles in cell lines used in Figure 1. (*A*) Human *DIS3L2* Exon 2 reference sequence (top) and alleles represented in DIS3L2 knockout clones (*bottom*). (*B*) Mouse *Dis3l2* Exon 3 reference sequence (*top*) and allele detected in mouse ES cell knockout clone (*bottom*). Note that in HeLa, Huh7, and E14tg2a, only a single allele was detectable at the DNA level, suggesting a homozygous mutation or a larger deletion that extended beyond the amplicon used for sequencing. In all cases, DIS3L2 was undetectable at the protein level.

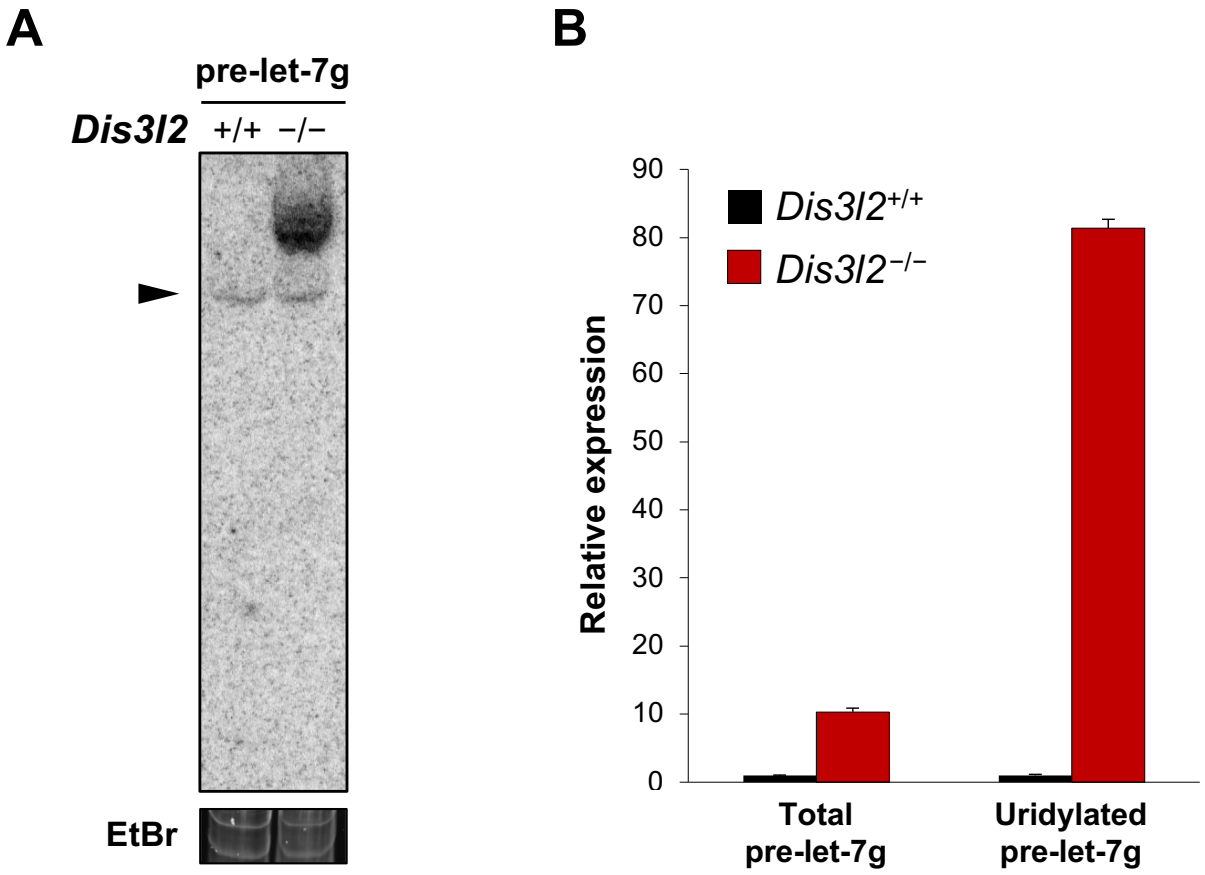

Supplemental Figure S3. **Loss of DIS3L2 in mouse embryonic stem cells leads to accumulation of uridylated pre-let-7g.** (*A*) Northern blot analysis of RNA from *Dis3l2* wild-type and knockout E14tg2a cells probed with an oligonucleotide complementary to the pre-let-7g terminal loop. Arrowhead marks expected migration of unmodified pre-let-7g. (*B*) qRT-PCR in E14tg2a cells measuring either total pre-let-7g (including both unmodified and tailed species) or uridylated pre-let-7g. Error bars represent standard deviation of technical triplicates.

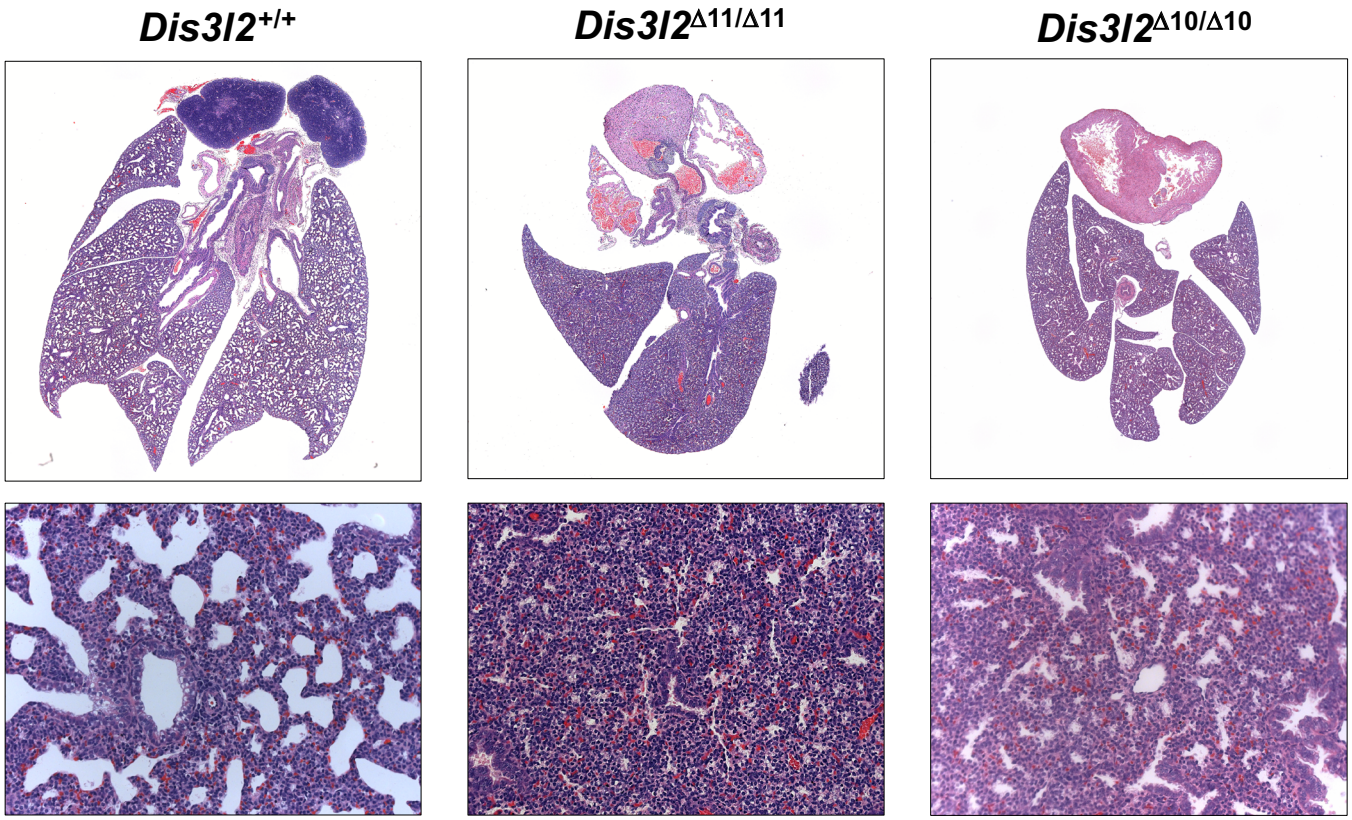

Supplemental Figure S4. **Underinflated lungs in *Dis3l2*-mutant mice.** H&E-stained sections of lungs taken from E18.5 caesarean-delivered embryos at low (*upper*) and high (*lower*) magnification.

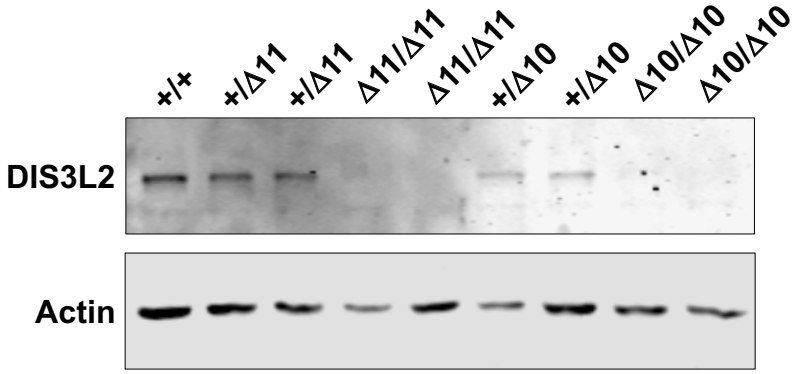

Supplemental Figure S5. DIS3L2 protein levels in E18.5 kidneys. Western blotting of whole kidney lysates from E18.5 embryos of the indicated genotypes.

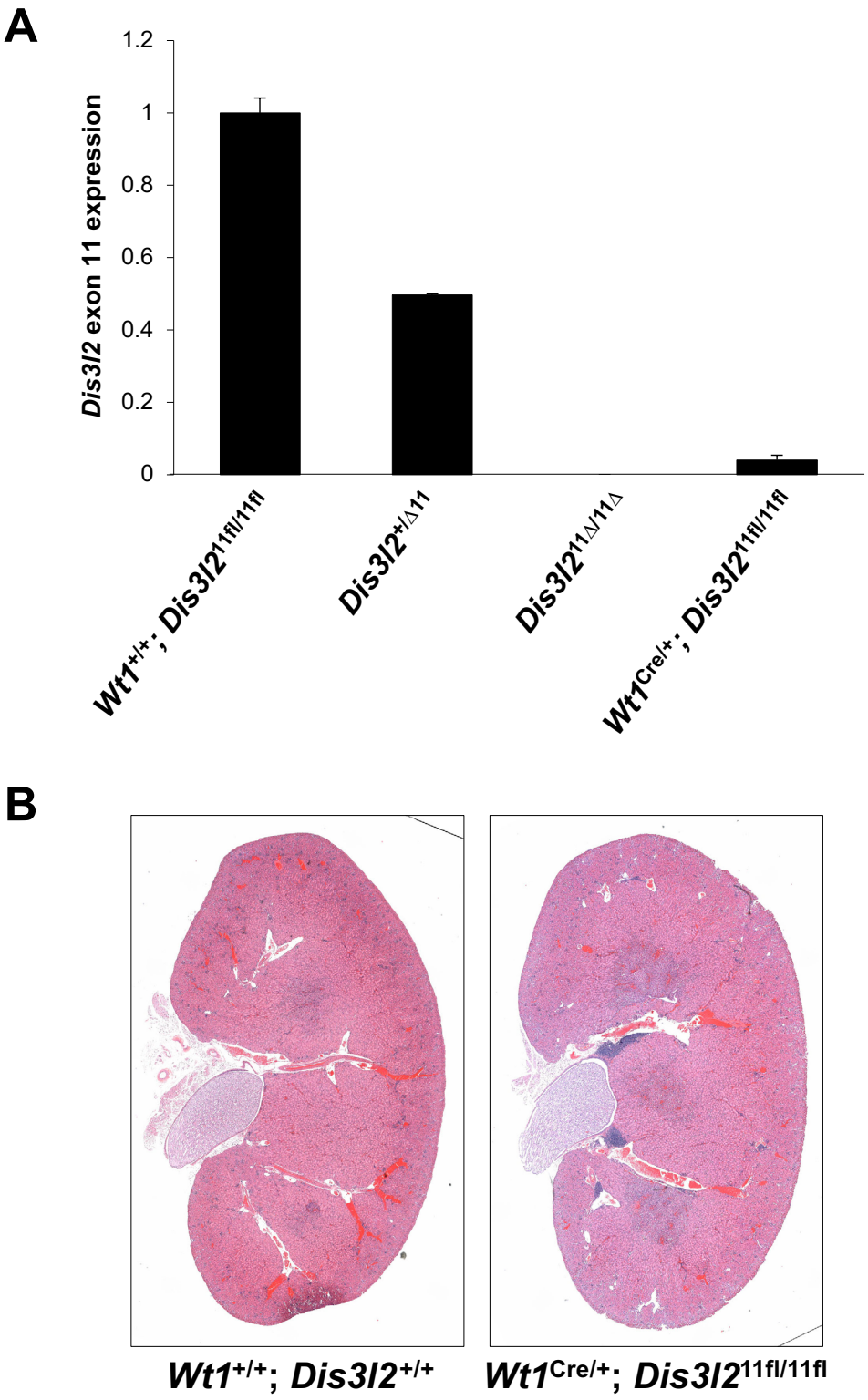

Supplemental Figure S6. Conditional deletion of *Dis3l2* in the kidney. (*A*) qRT-PCR measurements of exon 11-containing *Dis3l2* mRNA normalized to 18S in mice of the indicated genotypes. (*B*) H&E-stained sections of kidneys from 6 month-old littermates. Images are representative of $n = 21$ $Wt1^{Cre/+}$; $Dis3l2^{11fl/11fl}$ mice and $n = 21$ littermate controls ($Wt1^{+/+}$;$Dis3l2^{+/+}$, $Wt1^{Cre/+}$;$Dis3l2^{+/+}$, $Wt1^{+/+}$;$Dis3l2^{+/11fl}$, $Wt1^{Cre/+}$;$Dis3l2^{+/11fl}$, or $Wt1^{+/+}$;$Dis3l2^{11fl/11fl}$).

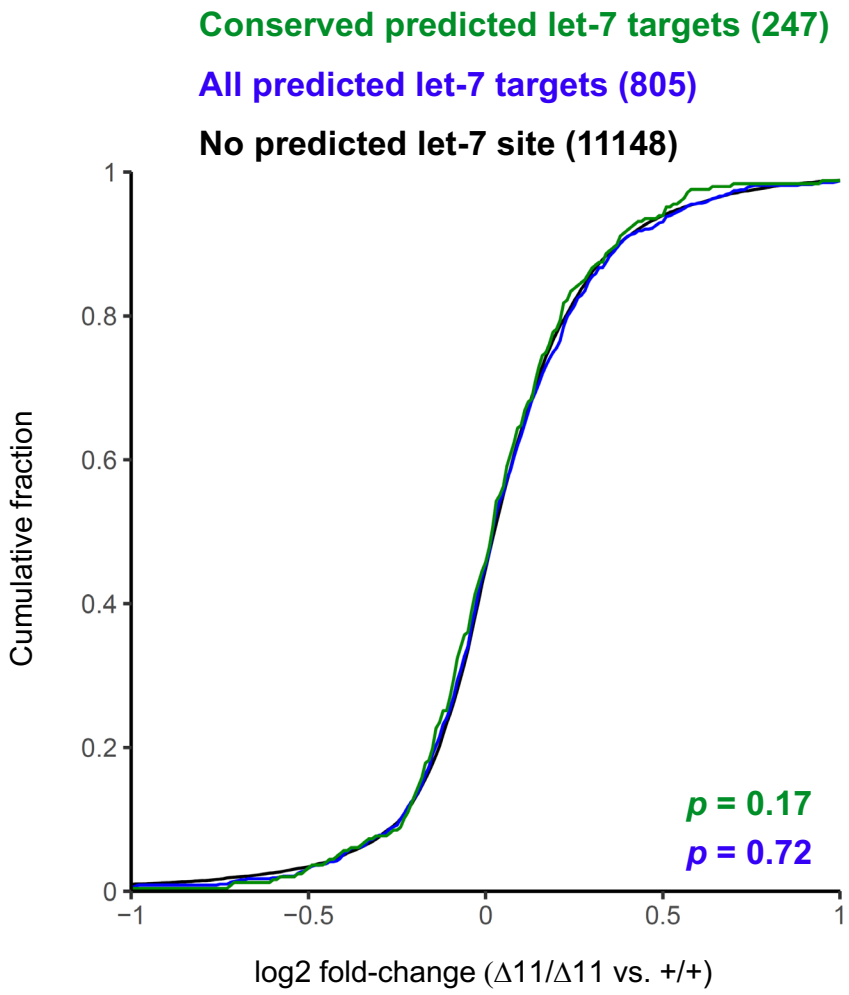

Supplemental Figure S7. **Analysis of let-7 target expression in *Dis3l2*$^{\Delta 11/\Delta 11}$ NPCs.** Predicted targets of mouse let-7 were obtained from Targetscan7.1 (www.targetscan.org/mmu_71/). The graph shows the cumulative distribution of fold-changes of conserved predicted let-7 targets (green), all predicted let-7 targets (blue), or mRNAs not predicted to be targeted by let-7 (black) in *Dis3l2*$^{\Delta 11/\Delta 11}$ vs. *Dis3l2*$^{+/+}$ NPCs. Only protein-coding genes expressed at or above 1 transcript per million (TPM) in at least one experimental sample were included in the analysis. *p* values, comparing each set of predicted targets to genes without a predicted let-7 binding site, were calculated using the Kolmogorov-Smirnov test.

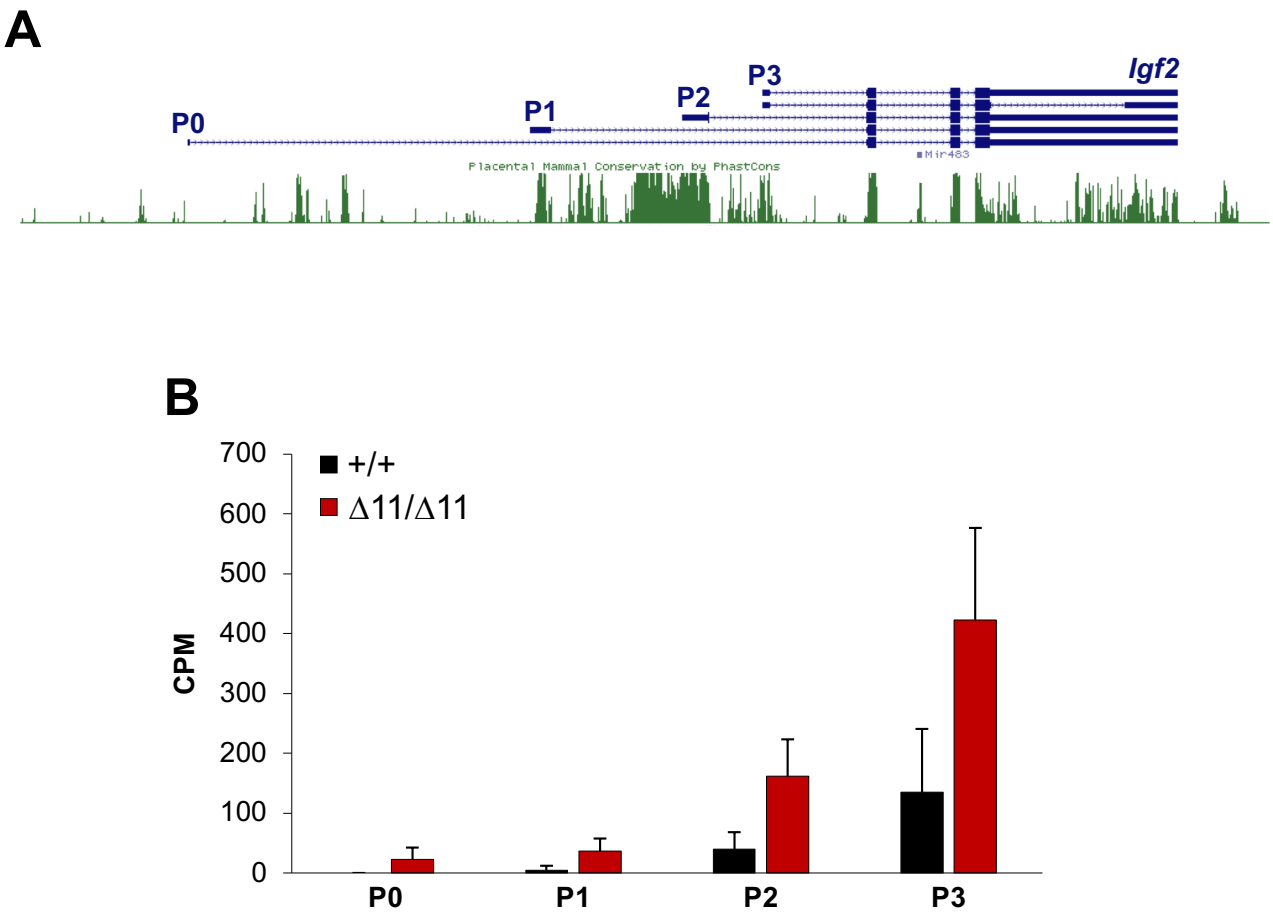

Supplemental Figure S8. **Relative *Igf2* promoter usage in *Dis3l2*$^{+/+}$ and *Dis3l2*$^{\Delta 11/\Delta 11}$ NPCs.** (*A*) UCSC Genome Browser screen shot showing location of mouse *Igf2* promoters and placental mammal conservation (mm10). (*B*) Relative promoter usage, determined by counting the number of RNA-seq reads spanning each promoter-specific exon and the first common exon of *Igf2*.

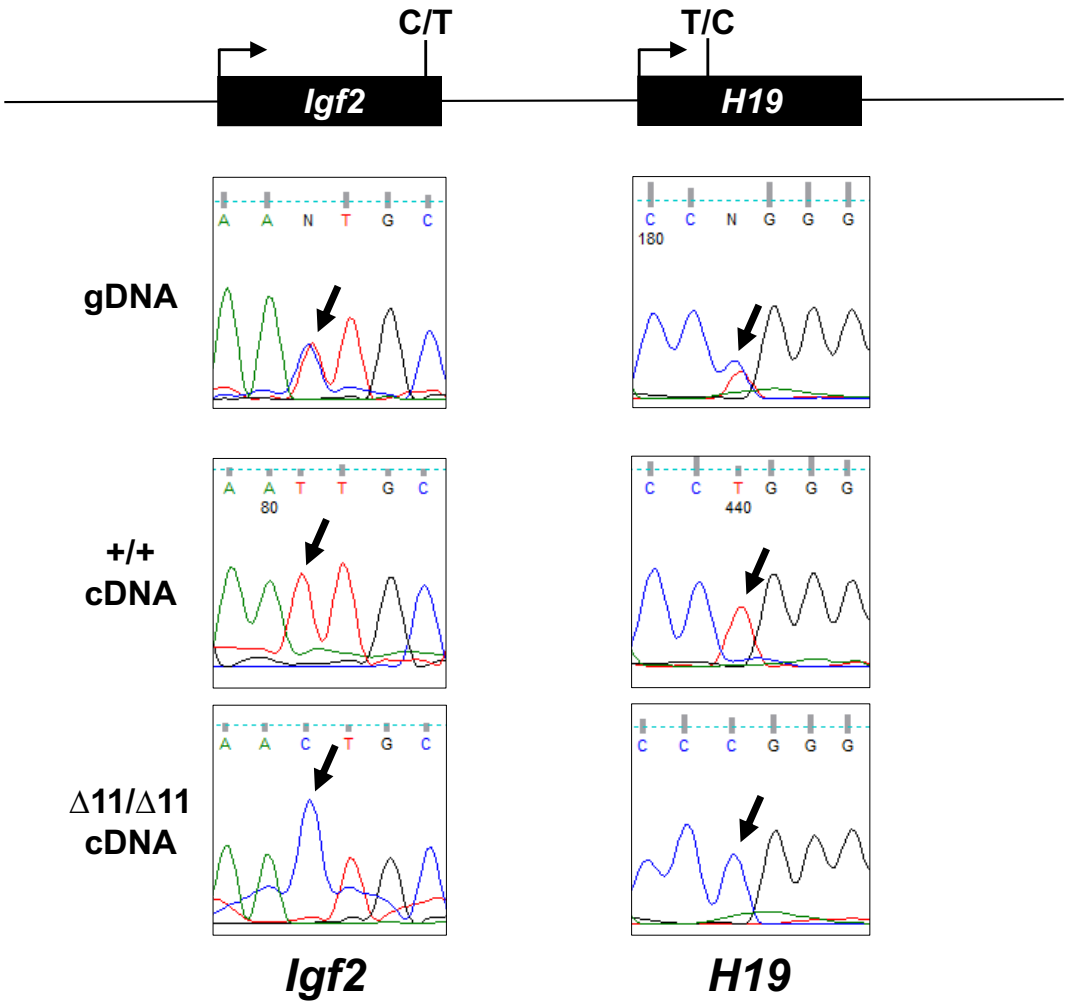

Supplemental Figure S9. **Imprinting of the *Igf2/H19* locus is preserved in *Dis3l2*$^{\Delta 11/\Delta 11}$ NPCs.** SNPs at the *Igf2/H19* locus (*top*) were used to confirm monoallelic expression of each gene in *Dis3l2*$^{+/+}$ and *Dis3l2*$^{\Delta 11/\Delta 11}$ NPCs by Sanger sequencing of amplified cDNA (*lower*).